JTTEE5 20:227–233
DOI: 10.1007/s11666-010-9545-5
1059-9630/$19.00 © ASM International

Peer Reviewed

Characterization of High-Temperature Abrasive Wear of Cold-Sprayed FeAl Intermetallic Compound Coating

Chang-Jiu Li, Hong-Tao Wang, Guan-Jun Yang, and Chong-Gao Bao

(Submitted May 14, 2010; in revised form July 27, 2010)

FeAl intermetallic compound coating was prepared by cold spraying using a mechanically alloyed Fe(Al) alloy powder followed by post-spray annealing at 950 °C. The high-temperature abrasive wear test was carried out for the FeAl coating at a temperature range from room temperature to 800 °C. The high-temperature abrasive wear of a heat-resistant stainless steel 2520 was performed for comparison. It was observed that the abrasive wear weight loss of FeAl coating was proportional to wear cycles in terms of sample revolutions at the tested temperatures. It was found that with the increase of the test temperature higher than 400 °C, the wear rate of cold-sprayed FeAl coating decreased with the increase of test temperature, while the wear rate of the heat-resistant steel increased significantly. The results indicate that the high-temperature abrasive wear resistance of the cold-sprayed FeAl intermetallic coating increased with the increase of the wear temperature in a temperature range from 400 to 800 °C. The wear resistance of cold-sprayed FeAl coating was higher than that of heat-resistant 2520 stainless steel under 800 °C by a factor of 3.

Keywords abrasive and erosive wear, cold gas dynamic spraying, wear mechanisms

1. Introduction

FeAl intermetallic compound is a promising structural material for several industrial applications from medium to high temperatures (Ref 1-3), due to their attractive properties such as high specific strength (strength-to-density ratio), high specific stiffness (stiffness-to-density ratio), good wear resistance, and excellent high-temperature corrosion resistance in oxidizing and sulfidizing atmospheres (Ref 4, 5). Moreover, Fe and Al, which are raw materials of FeAl phase, are relatively inexpensive, and the FeAl intermetallic alloy is lighter than steels or Ni-based alloys (Ref 3). Therefore, FeAl alloy is a potential alternative material for stainless steels or Ni-based superalloys in applications requiring high-temperature oxidation and sulfidation resistance, such as heating elements, furnace fixtures, and piping for fossil energy applications (Ref 4-6). However, with FeAl compound, as in the case of other intermetallics, the industrial application of this alloy has been limited due to its relatively low room-temperature ductility caused by environmental embrittlement, weak grain boundary bonding, and vacancy hardening (Ref 7). Although these problems can be alleviated to some degree by appropriate alloying element additions, it has proven difficult to formulate an alloy with both good creep resistance and low-temperature ductility.

In order to utilize its excellent wear and corrosion resistance at elevated temperature in the form of coating, several thermal spraying processes, such as plasma spraying (Ref 8), high-velocity oxy-fuel (HVOF) (Ref 6, 9), and wire-arc spraying (Ref 10), have been used to deposit FeAl alloys onto carbon steels and stainless steels for better corrosion protection. However, some deleterious effects inherent to conventional thermal spraying due to the high temperature would degrade the coating properties. For example, the oxidation of spray powders during conventional thermal spray processes would result in oxidation and oxide inclusions in the subsequent coating and deteriorate the overall wear and corrosion resistances (Ref 11). In addition, high residual tensile stress existing in the conventional thermally sprayed coating may cause unacceptable distortions, which significantly weakens the bond strength, accelerates fatigue failures, introduces microcracking, and reduces the performance of the coating (Ref 12).

This article is an invited paper selected from presentations at the 2010 International Thermal Spray Conference and has been expanded from the original presentation. It is simultaneously published in *Thermal Spray: Global Solutions for Future Applications, Proceedings of the 2010 International Thermal Spray Conference*, Singapore, May 3-5, 2010, Basil R. Marple, Arvind Agarwal, Margaret M. Hyland, Yuk-Chiu Lau, Chang-Jiu Li, Rogerio S. Lima, and Ghislain Montavon, Ed., ASM International, Materials Park, OH, 2011.

Chang-Jiu Li, Guan-Jun Yang, and **Chong-Gao Bao**, State Key Laboratory for Mechanical Behavior of Materials, School of Materials Science and Engineering, Xi'an Jiaotong University, Xi'an 710049, Shaanxi, China; and **Hong-Tao Wang**, School of Mechanical and Materials Engineering, Jiujiang College, Jiujiang 332005, Jiangxi, China. Contact e-mail: licj@mail.xjtu.edu.cn.

Recently, cold spraying has been widely investigated owing to its capability to deposit many oxygen-sensitive pure metallic or composite coatings (Ref 13-15). The major difference between the cold spray process and the conventional thermal spray processes is that the feedstock material does not experience molten or partially molten state during in-flight, since cold-sprayed deposits are formed through intensive plastic deformation of impacting particles in a solid state at a temperature well below the melting point of spray materials. Consequently, the deleterious effects inherent to conventional thermal spraying such as oxidation can be minimized or eliminated (Ref 13). This low-temperature characteristic of cold spraying makes it advantageous to deposit high performance FeAl alloys coating without composition change and property degradation. However, it may be difficult to deposit FeAl intermetallic coating directly using the intermetallic compound powder feedstock due to the intrinsic brittleness of intermetallic compounds at low temperature. Our previous study (Ref 16) showed that a dense FeAl intermetallic compound coating can be prepared by cold spraying using the ball-milled Fe(Al) solid solution alloy powder assisted with post-spray annealing treatment at a temperature of 500 °C.

Some investigations showed that FeAl intermetallic compound exhibited promising potential in severe wear and erosion conditions due to its high hardness, work-hardening rate, and good oxidation and corrosion resistance (Ref 17-19). The excellent high-temperature abrasive wear performance of the cold-sprayed FeAl coating was confirmed in our previous article (Ref 20). In this article, the high-temperature wear behaviour of cold-sprayed FeAl was further examined through weight loss change against the repeatitive wear cycle and the effect of environmental temperature on the wear rate of cold-sprayed FeAl.

2. Materials and Experimental Procedure

2.1 Feedstock Powder Preparation

The commercially available Fe and Al powders were used as starting materials to produce a composite feedstock powder with a composition corresponding to Fe60Al40 by ball milling, and the detailed milling process can be found in literature (Ref 16). Figure 1 shows typical surface morphology (Fig. 1a) and cross-sectional microstructure (Fig. 1b) of the as-milled powder for 36 h which was employed for coating deposition. The as-milled powder presented an irregular morphology. It can be seen from Fig. 1(b) that a fine lamellar structure is present in the powder. Two distinguishable regions with different microstructural characteristics can be clearly observed. Table 1 shows the high temperature abrasive wear test conditions.

2.2 Coating Preparation and Annealing Treatment

The cold spray system (CS-2000, Xi'an Jiaotong University) which consists of nozzle, gas heater, and high pressure gas supply unit was used for coating deposition. The setup of the system has been described in detail elsewhere (Ref 15). Spray particles were accelerated through a De Laval type of nozzle of 100 mm long with a circular cross section with an exit diameter of 6 mm and a throat diameter of 2 mm. The cold spray parameters are shown in Table 2. In this study, heat-resistant 2520 stainless steel (Fe55Cr25Ni20) with a hardness of 198 ± 11 Hv was used as a substrate material. Before spraying, the substrate surface was cleaned using acetone and sand-blasted using 24-mesh alumina grits. During deposition, the gun was manipulated by a robot at a traverse speed of 40 mm/s relative to the substrate. The as-sprayed coating was then annealed at 950 °C for 5 h in a tubular furnace in an argon atmosphere.

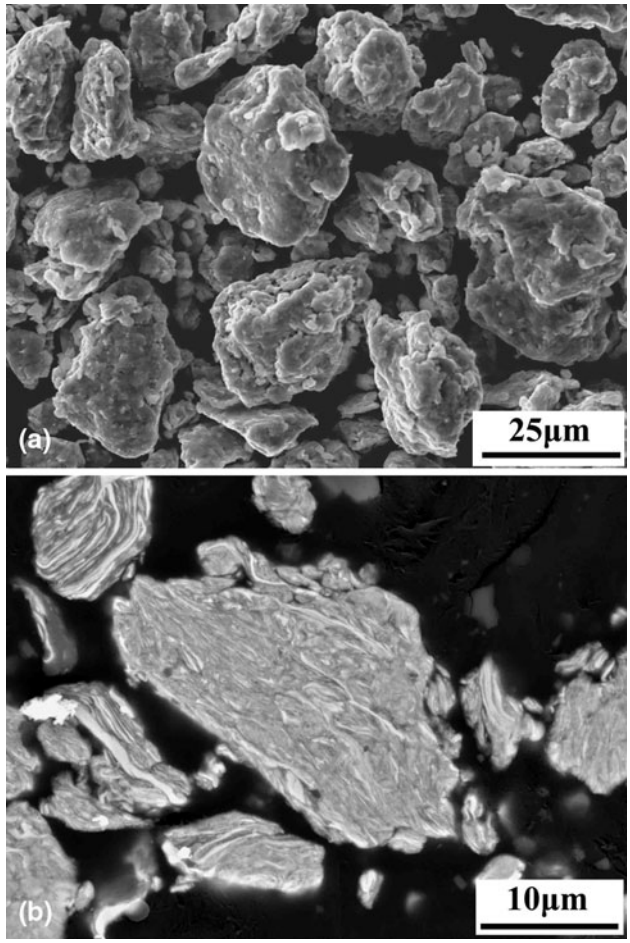

Fig. 1 Morphology (a) and cross-sectional microstructure (b) of the as-milled Fe/Al powder milled for 36 h

Table 1 High temperature abrasive wear test parameters

Rotation velocity, rpm	90
Rotation number, R	500, 1000, 1500, 2000, 2500
Abrasives flow, g/min	20.9
Load, N	19.6
Atmosphere	Air

Table 2 Cold spray parameters

Accelerating gas	N_2
Powder carrying gas	N_2
Accelerating gas pressure, MPa	2.0
Powder carrying gas pressure, MPa	2.5
Accelerating gas temperature, °C	500
Standoff distance, mm	20

2.3 Powder and Coating Characterization

The powder feedstock, the as-sprayed coatings, and the annealed coating were characterized by scanning electron microscopy (SEM, Quanta 200, FEI, Czechoslovakia) equipped with energy dispersive x-ray analysis (EDXA).

2.4 High-Temperature Abrasive Wear Test

The wear test was performed on a high-temperature three-body abrasive wear tester. The details about the tester and the wear test procedure can be found in literature (Ref 21). The shape of the upper specimen was a ring with a rectangular slot, and that of lower specimen is a disk. The upper and lower specimens were made from 2520 heat-resistant stainless steel and 1Cr18Ni9Ti stainless steel with a hardness of 201 ± 8 Hv, respectively. The upper specimen was used as substrate, and the coating with a thickness of 250 μm was deposited on its end face. For comparison, some upper specimens without coating were also tested. Under an applied load, the upper specimen (ring) was pressed against the lower specimens (disk), which was fixed on a spindle driven by a motor. During the test, the abrasives passing through a hollow shaft and a slot at the bottom of upper specimen were fed into the gap between the upper and lower specimens. Thus, the fresh abrasives act against the surfaces of counterparts subjected to wear. The wear test was carried out at different temperatures. After testing for 500 cycles, specimens were rinsed in alcohol, cleaned ultrasonically, dried, and weighed with a precision within ±0.1 mg. Five tests were performed on each sample. The wear rates were estimated as the slope of the cumulative coating weight loss curve against revolutions of the wear disk. The surface morphology of the coating after wear test was examined by SEM. The alumina grits of 100 mesh in size was used as abrasives.

3. Results and Discussion

3.1 Microstructure of the As-Sprayed Coating

Figure 2 shows the typical microstructure of the as-sprayed Fe/Al alloy coating in the SEM backscattered mode. It was clear from Fig. 2(a) that the as-sprayed Fe/Al coating presented a dense microstructure due to tamping effect of the deposited particles during cold spraying (Ref 15). Some thicker layers with a light gray contrast appeared in the coating microstructure shown in Fig. 2(b). According to previous results (Ref 16), the thicker layer was a Fe-rich phase and the fine lamella was

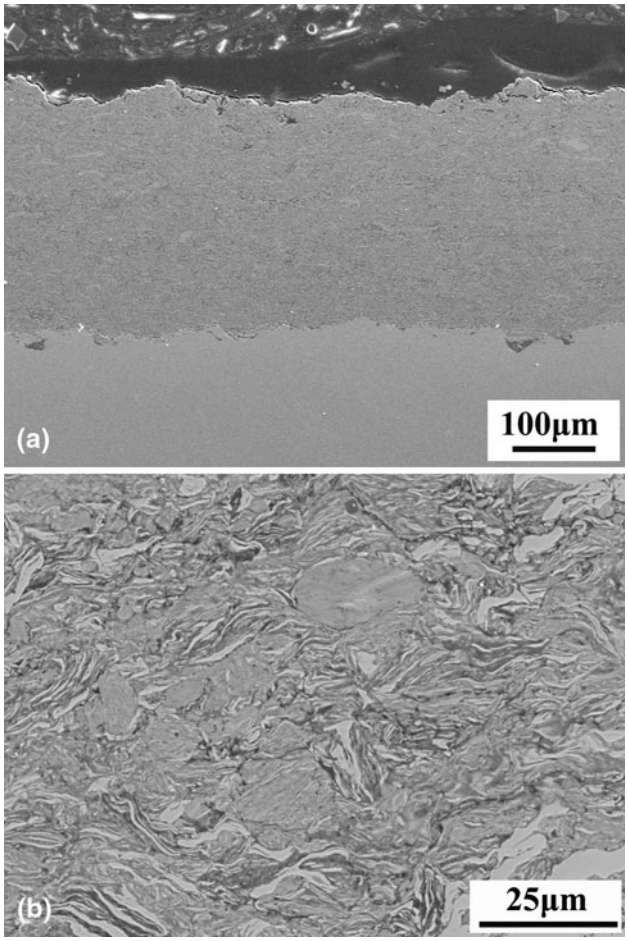

Fig. 2 Cross-sectional microstructure of the as-sprayed FeAl coating: (a) low magnification; (b) high magnification in SEM backscattered mode

a Fe-Al solid solution with high Al content. Moreover, from Fig. 2(b), it was noticeable that the lamellar microstructure of this coating was much finer than that of the cold-sprayed coating using the Fe and Al powder mixture (Ref 22). For the cold-sprayed coating using the Fe and Al powder mixture, the lamellar microstructure was developed by the particle deformation upon the high velocity impact (Ref 22). However, the lamellar structure in this study was developed not only from the particle deformation but also from the inner microstructure of the milled powder. Such microstructure features make it difficult to distinguish an individual single deformed particle boundary from the inner lamella interfaces in the coating.

3.2 Microstructure of the Annealed FeAl Coating

The previous results (Ref 16) indicated that the phase in the as-sprayed coating was Fe(Al) solid solution and the annealing treatment at 500 °C can realize the complete transformation of Fe(Al) solid solution to FeAl intermetallic compound. On the other hand, it is well known that the annealing treatment of thermally sprayed deposits can release residual stress, decrease the porosity, and modify

the microstructure and improve properties of the coatings (Ref 23). It has been proven that annealing of cold-sprayed deposits such as Cu can significantly modify coating properties (Ref 24). Moreover, the as-sprayed Fe-Al coating exhibits high activity due to its nanostructure (Ref 16). Therefore, it was considered that the post-spray annealing treatment would not only incur the phase transformation from the Fe(Al) solid solution to FeAl intermetallic compound but also significantly modify the microstructure of the cold-sprayed coating and the bonding state between the deposited particles.

Figure 3 shows the microstructure of the cold-sprayed FeAl coating after annealing at 950 °C for 5 h in the SEM backscattered mode. It can be seen that the fine white and gray lamellar structure existed in the as-sprayed coating completely disappeared due to solid-state diffusion and the microstructure of the coating became homogeneous, which can be seen clearly in Fig. 3(b). This fact means that the heterogeneous feature in the as-sprayed deposit can be modified through post-annealing treatment of the coating and the diffusion in the coating would lead to the coating microstructure without particle interfaces. It is important to note in Fig. 3(b) that the annealed coating was composed of a uniform FeAl phase with a small amount of Al_2O_3 particulates dispersed and a fully dense FeAl was achieved. In addition, a diffusion layer was observed at the interface between FeAl coating and substrate, in the same way as was found during annealing treatment of the cold-sprayed FeAl/Al_2O_3 coating (Ref 25).

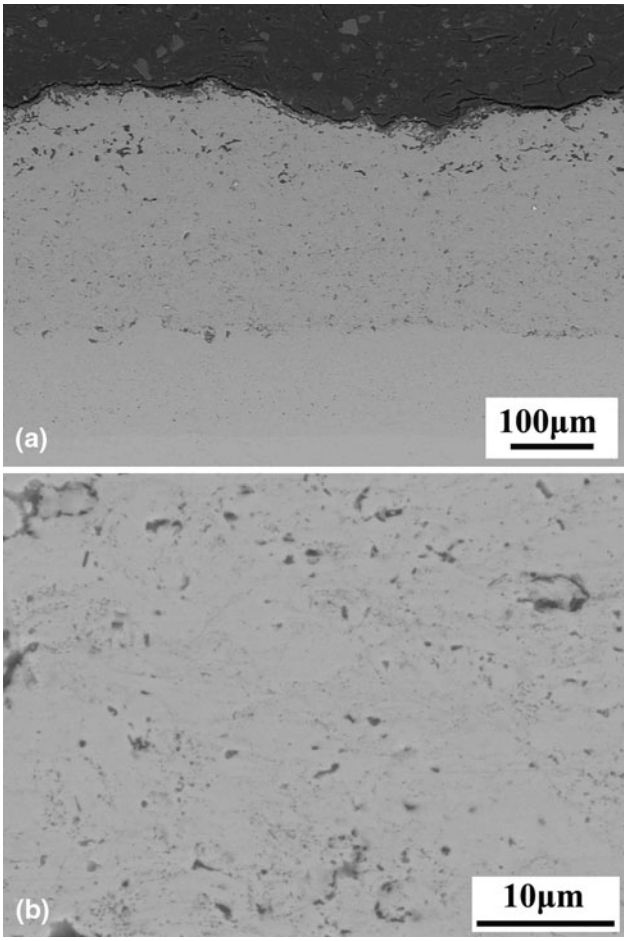

Fig. 3 Typical microstructure of the annealed FeAl coating: (a) low magnification; (b) high magnification

3.3 Effect of Temperature on Abrasive Wear Performance of Cold-Sprayed FeAl Coating

The increase of the total weight loss of cold-sprayed FeAl coating with the increase of revolutions of specimen at different wear test temperatures is shown in Fig. 4(a). It is clear that the weight loss of cold-sprayed FeAl coating tested at all temperatures increased linearly with the increase of the revolutions. This fact means that the high-temperature abrasive wear of the FeAl coating occurs steadily at a constant wear rate. Figure 4(b) shows the increase of the total weight loss of 2520 heat-resistant stainless steel with the increase of revolutions at different wear test temperatures. The wear weight loss of 2520 heat-resistant stainless steel increased also linearly with the increase of revolutions at different test temperatures. According to above results, the wear rate was estimated in terms of weight loss per unit rotation of wear counter disk.

Figure 5 shows the effect of test temperature on the wear rate of cold-sprayed FeAl coating (Fig. 5a) and 2520

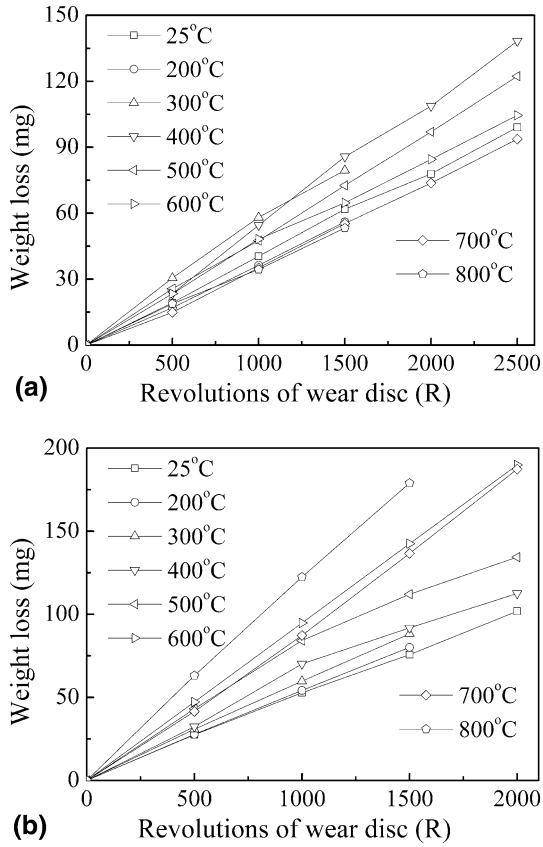

Fig. 4 Weight loss vs. revolution of counter disk tested at different temperatures for the cold-sprayed FeAl coating (a) and 2520 heat-resistant stainless steel (b)

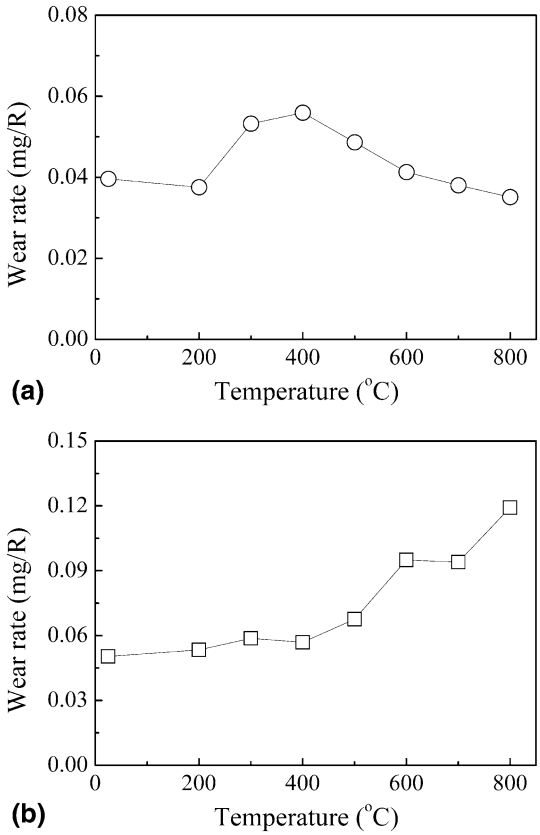

Fig. 5 Wear rate of cold-sprayed FeAl coating (a) and 2520 stainless steel (b) against the wear test temperature

stainless steel (Fig. 5b) as well. It can be clearly recognized that the dependence of wear rate of FeAl coating on test temperature is significantly different from 2520 heat-resistant stainless steel. As the temperature was increased to over 400 °C, the wear rate of 2520 stainless steel increased significantly with the increase of test temperature (Fig. 5b). This is possibly due to decrease in the microhardness of the stainless steel with the increase of temperature. It can be clearly seen from Fig. 5(a) that the wear rate of the FeAl coating increased as the test temperature increased from 200 to 400 °C. However, the wear rate of cold-sprayed FeAl coating decreased with increasing temperature in the temperature range from 400 to 800 °C, as shown in Fig. 5(a). Evidently, for example, the wear rate of the coating at a temperature of 500 °C was lower than that at 400 °C, and wear rate of the coating at 800 °C became comparable to that at room temperature. Such wear performance can be attributed to the anomalous strengthening behaviour of the cold-sprayed FeAl coating. Based on the test results as shown in Fig. 5, it can be recognized that the wear rate of 2520 stainless steel at 800 °C was more than three times that of the cold-sprayed FeAl coating. This fact indicates that the cold-sprayed FeAl coating is a promising candidate for the application to protect materials from high-temperature wear.

The investigations (Ref 26-28) show that many ordered intermetallic compounds such Ni_3Al, TiAl, Fe_3Al, and FeAl exhibit a feature known as the ''anomaly of the yield stress,'' which is characterized by a constant or increasing of value of the yield stress in a certain high-temperature range, while the yield stress of most materials decreases with the temperature increase. With FeAl intermetallic compound, the peak of the yield stress was observed in a temperature range of 673-823 K (Ref 26). From Fig. 5(a), it can be seen that the wear rate of cold-sprayed FeAl coating at a temperature of about 600 °C significantly reduced compared with 400 °C, which is consistent with anomalous strengthening effect.

3.4 Surface Morphology of FeAl Coating After Wear Test

Figure 6 shows the morphologies of the worn cold-sprayed FeAl coating and 2520 stainless steel after abrasion test at room temperature and 700 °C, respectively. With 2520 stainless steel, the typical features of microcutting and plastic deformation mechanisms were evidently observed from the surface morphology after wear test at room temperature and 700 °C, as shown in Fig. 6(a) and (b). Microcutting effect of abrasive grains causes material to be directly worn off, and plastic deformation takes place by ploughing action of the abrasive particles. In addition, some of fractured alumina abrasive particles were embedded into the worn surface, as indicated by white arrows in Fig. 6(a).

The typical surface morphology of the cold-sprayed FeAl coating after abrasive test at two temperatures was shown in Fig. 6(c) and (d). It can be seen clearly that the morphology of the worn FeAl coating tested at room temperature was similar to that of the 2520 stainless steel. The extensive plastic deformation caused by ploughing of the abrasive particles was observed. Accordingly, the primary wear mechanisms are microcutting and microplowing, as shown in Fig. 6(c). In addition, ''roughening'' along the edges of the grooves was observed at some areas, indicative of matrix microfracture. However, the worn surface of the cold-sprayed FeAl coating tested at 700 °C was distinct and was relatively smoother than that of the coating tested at room temperature, as shown in Fig. 6(d). Detailed examinations revealed the limited microcutting and plastic deformation effects by abrasive particles at 700 °C, where excellent resistance to abrasive wear was achieved. Consequently, the cold-sprayed FeAl coating exhibits the excellent high-temperature wear resistance, and such a temperature strengthening effect would expand the range of temperature for practical application of FeAl coating.

4. Conclusions

A dense FeAl intermetallic compound coating was deposited by cold spraying of mechanically alloyed powder assisted with post-spray annealing treatment.

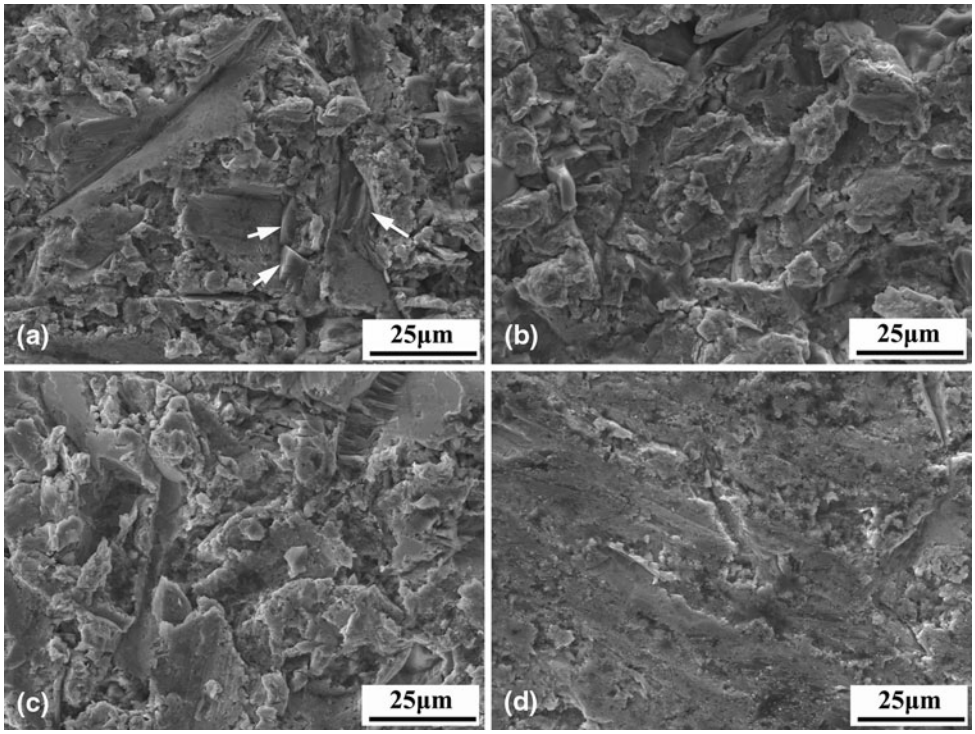

Fig. 6 Typical surface morphology of the cold-sprayed FeAl coating and 2520 heat-resistant stainless steel after wear test at RT and 700 °C: (a) stainless steel and RT; (b) stainless steel and 700 °C; (c) FeAl coating and RT; (d) FeAl coating and 700 °C

The high-temperature abrasive wear weight loss of the annealed cold-sprayed FeAl was proportional to wear cycles at the temperature range from room temperature to 800 °C. Accordingly, wear of the FeAl coating occurs at certain wear rate at certain temperature. The wear rate of the 2520 heat-resistant stainless steel increased significantly with the increase of the test temperature at the temperature higher than 400 °C, while the wear rate of the cold-sprayed FeAl coating tended to decrease with the increase of the abrasive wear test temperature from 400 to 800 °C. The wear resistance of cold-sprayed FeAl coating was higher than that of heat-resistant 2520 stainless steel under 800 °C by a factor of 3. The examination of the surface morphology of the coating after wear test suggests that microcutting is a dominant abrasive wear mechanism for cold-sprayed FeAl coating.

Acknowledgments

This study is supported by the National Science Fund for Distinguished Young Scholars (grant No. 50725101) and the Key Project of the Ministry of Education of China (No. 106145).

References

1. V.K. Sikka, J.T. Mavity, and K. Anderson, Processing of Nickel Aluminides and Their Industrial Applications, *Mater. Sci. Eng. A*, 1992, **153**(1-2), p 712-721
2. C.C. Koch, Intermetallic Matrix Composites Prepared by Mechanical Alloying—A Review, *Mater. Sci. Eng. A*, 1998, **244**(1), p 39-48
3. M. Krasnowski and T. Kulik, Nanocrystalline FeAl Intermetallic Produced by Mechanical Alloying Followed by Hot-pressing Consolidation, *Intermetallics*, 2007, **15**, p 201-205
4. C.T. Liu, E.P. George, P.J. Maziasz, and J.H. Schneibel, Recent Advances in B2 Iron Aluminide Alloys: Deformation, Fracture and Alloy Design, *Mater. Sci. Eng. A*, 1998, **258**(1-2), p 84-98
5. K. Natesan, Corrosion Performance of Iron Aluminides in Mixed-Oxidant Environments, *Mater. Sci. Eng. A*, 1998, **258**(1-2), p 126-134
6. C. Totemeier, R.N. Wright, and W.D. Swank, Microstructure and Stresses in HVOF Sprayed Iron Aluminide Coatings, *J. Therm. Spray Technol.*, 2002, **11**(3), p 400-408
7. N.S. Stoloff and C.T. Liu, Environmental Embrittlement of Iron Aluminides, *Intermetalics*, 1994, **2**(2), p 75-87
8. S. Kumar, V. Selvarajan, P.V.A. Padmanabhan, and K.P. Sreekumarand, Characterization and Comparison Between Ball Milled and Plasma Processed Iron-Aluminium Thermal Spray Coatings, *Surf. Coat. Technol.*, 2006, **201**(3-4), p 1267-1275
9. T. Grosdidier, A. Tidu, and H.L. Liao, Nanocrystalline Fe-40Al Coating Prepared by Thermal Spraying of Milled Powder, *Scripta Mater.*, 2001, **44**(3), p 387-393
10. H. Pokhmurska, V. Dovhunyk, M. Student, E. Bielanska, and E. Beltowska, Tribological Properties of Arc Sprayed Coatings Obtained from FeCrB and FeCr-Based Powder Wires, *Surf. Coat.Technol.*, 2002, **151-152**, p 490-494
11. K. Dobler, H. Kreye, and R. Schwetzke, Oxidation of Stainless Steel in the High Velocity Oxy-Fuel Process, *J. Thermal. Spray Technol.*, 2000, **9**(3), p 407-413
12. T.W. Clyne and S.C. Gill, Residul Stresses in Thermal Spray Coatings and Their Effect on Interfacial adhension: A Review of Recent Works, *J. Thermal. Spray. Technol.*, 1996, **5**(4), p 401-418
13. A. Papyrin, Cold Spray Technology, *Adv. Mater. Process.*, 2001, **159**(9), p 49-51

14. R.C. McCune, W.T. Donlon, O.O. Popoola, and E.L. Cart-wright, Characterization of Copper Layers Produced by Cold Gas-Dynamic Spraying, *J. Therm. Spray Technol.*, 2000, **9**(1), p 73-82
15. C.-J. Li and W.-Y. Li, Deposition Characteristics of Titanium Coating in Cold Spraying, *Surf. Coat. Technol.*, 2003, **167**(2-3), p 278-283
16. H.-T. Wang, C.-J. Li, G.-J. Yang, C.-X. Li, Q. Zhang, and W.-Y. Li, Microstructural Characterization of Cold-Sprayed Nanostructured FeAl Intermetallic Compound Coating and Its Ball-Milled Feedstock Powders, *J. Therm. Spray Technol.*, 2007, **16**(5-6), p 669-676
17. G. Sharmaa, P.K. Limayeb, R.V. Ramanujanc, M. Sundararamana, and N. Prabhud, Dry-Sliding Wear Studies of Fe_3Al-Ordered Intermetallic Alloy, *Mater. Sci. Eng. A*, 2004, **386**(1-2), p 408-414
18. Y.S. Kim and Y.H. Kim, Sliding Wear Behavior of Fe_3Al-Based Alloys, *Mater. Sci. Eng. A*, 1998, **258**(1-2), p 319-324
19. G. Sharma, P.K. Limaye, M. Sundararaman, and N.L. Soni, Wear Resistance of Fe-28Al-3Cr Intermetallic Alloy Under Wet Conditions, *Mater. Lett.*, 2007, **61**(16), p 3345-3348
20. H.T. Wang, G.J. Yang, C.-J. Li, and C.G. Bao, Study of High-Temperature Abrasive Wear Performance of Cold-Sprayed FeAl Intermetallic Compound Coatings, *Mater. China*, 2009, **28**(2), p 61-64 (in Chinese)
21. J.D. Xing, Y.M. Gao, E.Z. Wang, and C.G. Bao, Effect of Phase Stability on the Wear Resistance of White Cast Iron at 800 °C, *Wear*, 2002, **252**(9-10), p 755-760
22. H.-T. Wang, C.-J. Li, G.-J. Yang, and C.-X. Li, Cold Spraying of Fe/Al Powder Mixture: Coating Characteristics and Influence of Heat Treatment on the Phase Structure, *Appl. Surf. Sci*, 2008, **255**(5), p 2538-2544
23. J.P. Schaffer, A. Saxena, S.D. Antolovich, T.H. Sanders, Jr., S.B. Warner, The Science and Design of Engineering Materials, 2nd ed., McGraw-Hill, OH (1999)
24. W.-Y. Li, C.-J. Li, and H.-L. Liao, Effect of Annealing Treatment on the Microstructure and Properties of Cold-sprayed Cu Coating, *Therm. Spray Technol.*, 2006, **15**(2), p 206-211
25. H.-T. Wang, C.-J. Li, G.-J. Yang, and C.-X. Li, Effect of Heat Treatment on the Microstructure and Property of Cold-sprayed Nanostructured $FeAl/Al_2O_3$ Intermetallic Composite Coating, *Vacuum*, 2008, **83**(1), p 146-152
26. K. Marian, High Temperature Strengthening of the FeAl Intermetallic Phase-Based Alloy, *Intermetallics*, 2006, **14**(2), p 149-155
27. M. Koeppe, C. Hartig, and H. Mecking, Anomalies of the Plastic Yield Stress in the Intermetallic Compound Fe-30 at.%Al, *Intermetallics*, 1999, **7**(3-4), p 415-422
28. Y. Yang, I. Baker, G.T. Gray, and C. Cady, The Yield Stress Anomaly in Stoichiometric FeAl at High Strain Rate, *Scripta Mater.*, 1999, **40**(4), p 403-408